COMPARATIVE ANALYSIS FOR PHASE IIA AND IIB EXPERIMENTS OF THE U.S./JAERI COLLABORATIVE PROGRAM ON FUSION BLANKET NEUTRONICS

M.Z. Youssef, Y.Watanabe, M. Abdou
Mechanical, Aerospace and Nuclear Engineering
University of California, Los Angeles
Los Angeles, CA 90024, U.S.A.
(213) 825-2879

M. Nakagawa, T. Mori, K. Kosako, T. Nakamura
Japan Atomic Energy Research Institute
Tokai-mura, Naka-gun, Ibaraki-ken, 319-11
JAPAN
011-81-(292) 82-5709

ABSTRACT

Several fusion-oriented integral experiments were performed in Phase II of the U.S./JAERI Collaborative Program on Fusion Neutronics where the geometrical configurations and source condition closely simulate the incident spectrum in fusion reactors. The main objective of the program is to estimate the uncertainties involved in predicting tritium breeding rate in Li_2O and other neutronics parameters in fusion blankets that include engineering features (i.e., first wall, multiplier). In Phase II, the Li_2O test assembly is placed on one end of a Li_2CO_3 enclosure that houses the D-T neutron source. Predicted local and integrated tritium production rates (TPR) from $^6Li(T_6)$, $^7Li(T_7)$ and natural lithium (T_N) were compared to measurements in various configurations that included reference, first wall and beryllium multiplier experiments (Phase IIA) in addition to repeating these experiments with a FW/Be layer covering the interior surface of the Li_2CO_3 enclosure (Phase IIB). Other neutronics parameters that included source characterization by foil measurements, in-system reaction rates, and in-system spectrum measurements were also analyzed. The analyses were carried out independently by both parties using various 3-D Monte Carlo codes and 2-D discrete ordinates codes and data libraries. The results of the analyses are reported in this paper with emphasis placed on the impact of the beryllium data on the discrepancies found between predictions and measurements.

I. INTRODUCTION

The prediction accuracy of tritium breeding in a fusion blanket is a prime design issue since a slight uncertainty in tritium breeding inside those breeders that have marginal tritium breeding capability could lead to not achieving tritium self-sufficiency, a costly penalty that requires reliance on an external tritium supply. For that purpose, an Integral Experiments Program has been initiated between the U.S. and JAERI to evaluate the overall uncertainties involved in breeding tritium inside a Li_2O test assembly. Several experiments have been conducted at the Fusion Neutron Source (FNS) facility at the Japanese Atomic Energy Research Institute (JAERI) with the objective of verifying the potential for tritium breeding in a simulated fusion blanket that has engineering features (e.g., first wall, multiplier) and making comparisons between analytical predictions and measurements to arrive at estimates for the uncertainties associated with tritium breeding as well as other neutronics parameters. The results obtained from this Program will provide a data base for selection of materials, blanket configuration, and the neutronics technology required for the next experimental device, such as FER, ITER, etc.

Phase I of the program has been completed and the results from that Phase have been reported elsewhere.[1-4] In contrast to Phase I, Phase II geometrical arrangements closely simulate the incident neutron spectrum on the Li_2O test assembly that is found in a fusion reactor.[5-8] The assembly is located at one end of a rectangular Li_2CO_3 enclosure which is isolated from the surroundings by a polyethylene layer. A water-cooled rotating neutron target (RNT) has been deployed to generate the intense 14 MeV neutron source and is located in the inner cavity of the Li_2CO_3 enclosure at a relatively short distance (~78 cm) from the Li_2O test assembly. In addition to simulating the incident neutron spectrum by careful selection of geometry and materials, Phase II experiments are also characterized by the extensive use of beryllium as a neutron multiplier and armor. The characteristics of the calculated-to-measured (C/E) curves of T_6 and T_7 (and other parameters) upon including Be in various configurations were used to infer the degree of accuracy of the beryllium nuclear data and its impact on neutron multiplication and tritium breeding in the Li_2O assembly.

II. THE EXPERIMENTS

Phase II consists of three types of experiments, namely, Phase IIA, Phase IIB, and Phase IIC experiments. The experiments considered in Phase IIA are (a) a reference Li_2O system: In this experiment the whole rectangular test zone (86 cm x 86 cm x 60 cm depth) is occupied by the Li_2O assembly constructed from Li_2O blocks of different sizes, the smallest of which is 5.06 cm x 5.06 cm x 5.06 cm. Figure (1) shows the test assembly and the rectangular Li_2CO_3 enclosure whose outer dimensions are ~ 126 cm x 126 cm x 225 cm and is ~ 20 cm thick. A 5-cm thick polyethylene (PE) layer surrounds the entire enclosure to isolate the test assembly from the room-returned neutrons that are reflected by the concrete walls of Room #2 (4.96 m x 4.96 m and 4.5 m height) where the experiments are performed. Two (central and off-central) drawers were installed throughout the axial direction of the test assembly where measurements are performed. In addition, two radial drawers were also installed at Z = 12.4 cm (front drawer) and at Z = 42.76 cm (back drawer) from the front surface of the assembly. (b) Be-front System: in this experiment, the front 5 cm of the Li_2O assembly was removed and replaced by an equivalent volume of beryllium blocks to study the impact of neutron multiplication in Be on the TPR profiles behind the multiplier. (c) Be-sandwiched system: in this experiment, a 5-cm-thick layer of Be was sandwiched between a front 5 cm-thick Li_2O layer and the rest of the Li_2O assembly, as shown in Fig. (1).

The TPR from ^6Li (T_6) and $^7Li(T_7)$ were measured by various methods (Li-glass detectors, Li-metal detectors, Li_2O-pellet detectors) along the axial and radial drawers. The T_7 was also measured by folding the measured spectrum with the response $^7Li(n,n'\alpha)t$ cross (NE213 indirect method). The in-system spectrum measurements were preformed by using small spherical NE213 in the energy range $E_n > 1$ MeV and by using a small size proton recoil counter (PRC) in the energy range 1 Kev < E_n < 1 MeV. Foil activation measurements along the axial drawers were performed in the reference and Be-sandwiched systems which included the reactions $^{58}Ni(n,2n)$, $^{58}Ni(n,p)$, $^{27}Al(n,\alpha)$, $^{93}Nb(n, 2n)$ ^{92m}Nb, $^{197}Au(n,2n)$, $^{115}In(n,n')^{115m}In$, and $^{197}Au(n,\gamma)$. Since the cross-sections for these reactions have different threshold energy and energy dependence, comparisons between

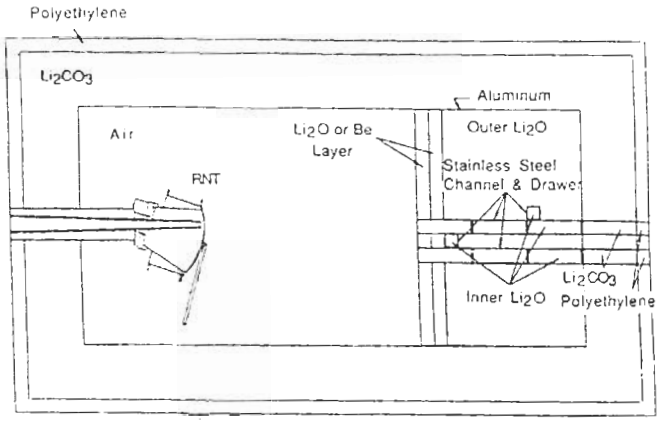

Fig. (1) The rotating neutron target, (RNT), the Li_2CO_3 enclosure and the Li_2O assembly of Phase II

measurements and calculations provide useful information on the neutronics characteristics inside the Li_2O assembly. Zonal TPR from natural lithium (T_N), ^7Li and ^6Li were also measured in several designated zones along the central drawer (5.08 cm x 5.08 cm x 60 cm) in the reference and the Be-sandwiched systems of Phase IIA. The experimentally-evaluated integrated TPR along the central drawer was then compared to the calculated values (indicative of tritium breeding ratio, TBR). In addition to performing the above-mentioned in-system measurements, the nuclear field inside the cavity, at the inner surface of the Li_2CO_3 enclosure, and at the front surface of the Li_2O assembly has been characterized by carrying out spectrum and foil activation measurements that included the reaction rates $^{58}Ni(n,2n)$, $^{58}Ni(n,p)$, $^{93}Nb(n,2n)$, $^{27}Al(n,\alpha)$, $^{197}Au(n,2n)$, and $^{197}Au(n,\gamma)$. These source characterization measurements were necessary to perform prior to Phase II experiments in order to estimate the uncertainties in predicting the incident neutron source to the Li_2O assembly.

In Phase IIB experiments, the interior surface of the Li_2CO_3 enclosure was covered by a 0.5 cm-thick SUS304 first wall (FW) followed by a 5 cm-thick beryllium liner and the reference and the Be-front experiments of Phase IIA were repeated. The Be-front experiments of Phase IIB were carried out with and without a 0.5 cm-thick FW. The objective of these experiments was to study the impact of including a Be liner (similar to the Be-tiles on the inboard shield of fusion reactors) on the breeding performance of the Li_2O assembly. The massive amount of beryllium utilized in Phase IIB enabled us to examine the accuracy of beryllium neutron cross-sections and the consequent impact on tritium breeding enhancement due to neutron multiplication in beryllium through the $^9Be(n,2n)$ reactions. The TPR from ^6Li in this phase was measured by the Li-glass on-line method while T_7 was measured by the NE213 indirect method. The T_6 and T_7 local values were also measured by the Li-metal and Li_2O-pellet detectors in the Be-front with FW experiment in addition to the in-system spectrum measurements by the NE213 and PRC.[9] Foil activation measurements were also performed in that phase to determine the incident neutron spectrum.[10]

Phase IIC experiments have not been performed yet but they are scheduled during the experimental period Oct. 15 - Dec. 15, 1988. These experiments are aimed at examining the heterogeneity effects (multilayers of Be and inclusion of several coolant channels inside the test zone) on the TPR and heating rates profiles.[11] Activities on that Phase will be reported separately.

III. CALCULATIONAL METHODS

Both deterministic and Monte Carlo methods were independently applied by the U.S. and JAERI in analyzing Phase II experiments. The MCNP[12] (version 3A) was used by the U.S. along with its pointwise continuous energy/angle cross-section library RMCCS/BMCCS based on ENDF/B-V data. The MORSE-DD code[13] (utilizes multi-group double differential form for neutron cross-section) has been used by JAERI in the Monte Carlo calculations along with the DDL/J3P1 library that is based on JENDL3-PR1 (125-g). In the 2-D calculations, the U.S. used the DOT 4.3 and DOT 5.1 discrete ordinates codes along with the MATXS6[14] cross-section library (ENDF/B-V, 80-g) and the LANL evaluation for ^7Li[15] and ^9Be[16]. The DOT 3.5 code was applied in the 2-D calculations performed by JAERI where the cross-section library adopted (125-g) is based on JENDL3-PR1 data.

In the source characteristics calculations, the U.S. has used the MORSE-CG code and a library consisting of 53-g cross-sections collapsed from the VITAMIN-E library was applied. The MORSE-DD code was also applied by JAERI for source characterization. The activation reaction rates inside the cavity were calculated by the ORACT[17] library in the U.S. calculations while in-system reaction rates were based on the activation reaction rates provided by the pointwise library of the MCNP code. JAERI has used activation data from ENDF/B-IV file as well as the recently measured cross-sections at the FNS by Ikeda et al.[18] In-system reaction rates obtained by the 2-D calculations were evaluated by the activation cross-section of ENDF/B-V (U.S.) and JENDL3-PR1 (JAERI), independently.

In the calculational model used in the Monte Carlo calculations performed by JAERI, neutron importance was varied according to the incident direction to the Li_2O assembly and the geometrical details of the target were considered as precisely as possible.[5] The model adopted by the U.S. in the MCNP calculations is similar. The assembly, the RNT and the Li_2CO_3 enclosure were modeled in cylindrical geometry in the 2-D calculations. The model adopted by the U.S. in DOT5.1 calculations is shown in Fig. (2) where part of the RNT target is shown and the D-T neutrons are emitted at the zero coordinates. The energy and angular distribution of neutrons produced at the beam spot (z=r=0) has been calculated based on the formula of Benveniste et al.[19] and on the D-T kinematics for the corresponding D^+ beam energy. Note that the FW/Be liner is shown in Fig. (2) for Phase IIB and is excluded from the calculations for Phase IIA, depending on what experiment is analyzed. In these calculations, the hydrogen-rich epoxy paint for the Li_2CO_3 blocks from which the enclosure was constructed was homogenized with the Li_2CO_3 material, as noted in the figure. Note also from the figure that the concrete walls of the room where the experiments were performed are included in the model with a thickness of ~60 cm which was judged adequate to represent the room effect.

IV. ANALYTICAL RESULTS AND COMPARISON WITH EXPERIMENTAL VALUES

IV.1 PHASE IIA

The analysis for Phase IIA has been previously reported[5-7] and we briefly discuss the important results for completeness and comparison with Phase IIB results. In characterizing the source inside the cavity by foil activation measurements, the prediction of $^{197}Au(n,2n)$ and $^{27}Al(n,\alpha)$ reaction rates at the inner surface of the Li_2CO_3 enclosure agree well with the measurements at the forward direction to the RNT but large deviations (~factor of 2) were observed at the locations behind the RNT due to inaccuracy in modeling the equipment that surrounds the RNT (e.g., a motor, position and composition of tubes containing cooling water, etc.). Neutrons generated with a flight path in the backward direction are scattered first by these components and inaccuracy in modeling these components considerably affects the calculated reaction rates at these back locations, which are sensitive to high energy neutrons, as shown in Fig. (3) for the $^{93}Nb(n,2n)$ reaction rates. Although JAERI's calculations for the $^{58}Ni(n,p)$ reactions that are based on ENDF/B-IV shows overestimation by 10-20%, the values obtained by the ORACT[17] library and by the new cross-section measured by Ikeda et al.[18] reduced the discrepancies to several percents.

In the case of $^{58}Ni(n,2n)$ reaction rate, the results based on ENDF/B-IV data and the ORACT library give smaller C/E values by about 10 and 30%, respectively, but Ikeda's cross-sections reduced the discrepancies to about 5%. Thus, the $^{58}Ni(n,2n)$ cross-sections that are currently implemented in ENDF/B-IV(and V) need re-evaluation.

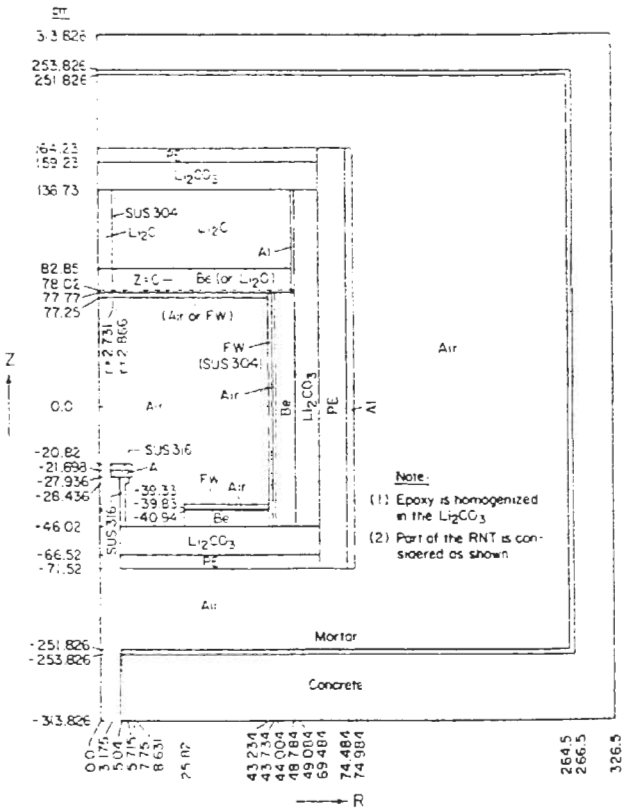

Fig. (2) The material and geometrical arrangement for Phase IIB used in 2-D model of DOT5.1 calculations (U.S.)

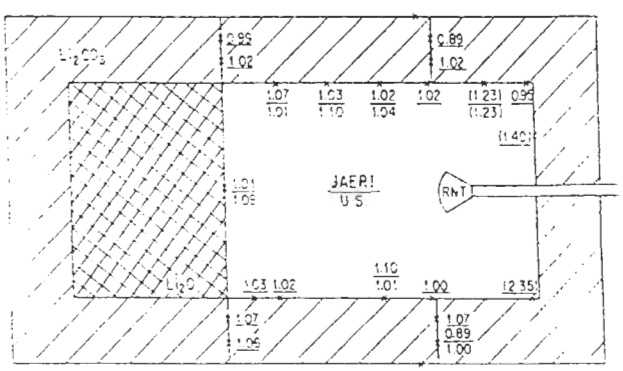

Fig. (3) The C/E values for the $^{93}Nb(n,2n)^{92}Nb$ reaction rate at the midplane of the system. X's show the measuring locations

To characterize the incident source to the test assembly, maps of several activation rates on the vertical and horizontal directions across the front surface of the Li_2O assembly were made. Fig. (4) shows the C/E values from $^{93}Nb(n,2n)$ reactions in the horizontal (L & R) and vertical (U & L) direction. It can be seen that the new cross-section of Ikeda et al. accurately predicts the measured values though the ENDF/B-IV data overestimates the reactions by several percent. It was concluded that the activation cross-sections of $^{58}Ni(n,2n)$, $^{58}Ni(n,p)$ and $^{93}Nb(n,2n)$ in ENDF/B-IV (and also B/V) mispredict the activation rates; on the other hand, those cross-sections measured at the FNS and those implemented in the ORACT file [except for $^{58}Ni(n,2n)$] significantly decrease the discrepancies found between measurements and calculated values.

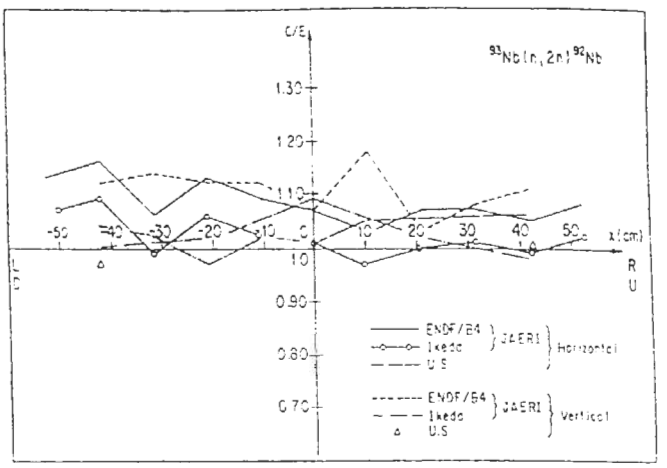

Fig. (4) The C/E values for the $^{93}Nb(n,2n)^{92}Nb$ reaction rate on the surface of the Li_2O assembly

IV.1.A TRITIUM PRODUCTION RATE FOR ^6LI (T_6)

In the reference system, T_6 is generally overestimated by all codes and libraries along the central axis of the Li_2O assembly where Li-glass detectors were used in the measurements. The C/E values ranged from 0.9 to 1.25 but in the bulk of the assembly, the C/E values are around 1.1 (experimental errors are ~3-4%). The discrepancy is large in the Li_2CO_3 layer due to the uncertainties in the specifications of the Li_2CO_3 blocks, e.g., atomic densities, epoxy paint content, etc. With the Li-metal detectors, the C/E values were closer to unity (1-1.1) but the overestimation still persists. The C/E values for T_6 in the radial directions were found to be ~1-1.1.

The effect of using beryllium as a neutron multiplier on T_6 profiles is that an enhancement occurs (by a factor of 2-3) in the local values at locations adjacent to the beryllium zone in both the Be-front and Be-sandwiched systems in comparison to the reference system. However, no noticeable increase in T_6 is observed at deep locations. In addition, T_6 values measured in the beryllium region are noticeably large (a factor of 8.5 , and 6 increase in the Be-sandwiched and Be-front systems, respectively) due to the fairly soft spectrum encountered inside the beryllium zone. The C/E values for T_6 are shown in Fig. (5) for the Be-front system. The values in the bulk of the Li_2O zone vary among various calculations and are ~0.8 - 1.1 but they are generally closer to unity in comparison to the reference system. However, large discrepancies are found in the beryllium zone and at locations near the Be-Li_2O boundary. The C/E values inside the beryllium are as large as 1.63 (MORSE/J3PR1) and 1.59 (MCNP/B5). Further analysis indicates that this discrepancy was due to the detector (Li-glass) self-shielding effect and to flux perturbation by the various components of the detector whose details were ignored in the calculational model , which amounts to 30% and 20% respectively.[6] Note also from Fig. (5) that there is a sudden drop in the C/E values behind beryllium (C/E~0.8 - 0.95). These features were also found in the Be-sandwiched system. The reasons for these features are discussed in Section IV.2 on Phase IIB. Also note from Fig. (5) that the C/E values in the beryllium zone as predicted by JAERI using the JENDL3-PR1 evaluation for beryllium are larger than those obtained by the U.S. using Young's evaluation.[16] Direct comparison for beryllium data[6] showed that $^9Be(n,total)$ and $^9Be(n,elastic)$ cross-sections are similar in the two evaluations; however, $^9Be(n,2n)$ cross-section is smaller in JENDL3-PR1 by ~3-5% than in Young's evaluation. In addition, when the secondary energy

distribution of the emitted neutrons of the $^{9}Be(n,2n)$ cross-section was examined, it was found that JENDL3-PR1 data has a larger slow neutrons component (E<0.5 MeV) in the forward direction than in Young's evaluation, which gives harder spectrum. This leads to a larger T_6 in JAERI's calculations although the total $^{9}Be(n,2n)$ cross-section is smaller by 3-4%. The harder spectrum in Young's evaluation leads to larger T_7 in the Be zone, as predicted by the U.S.

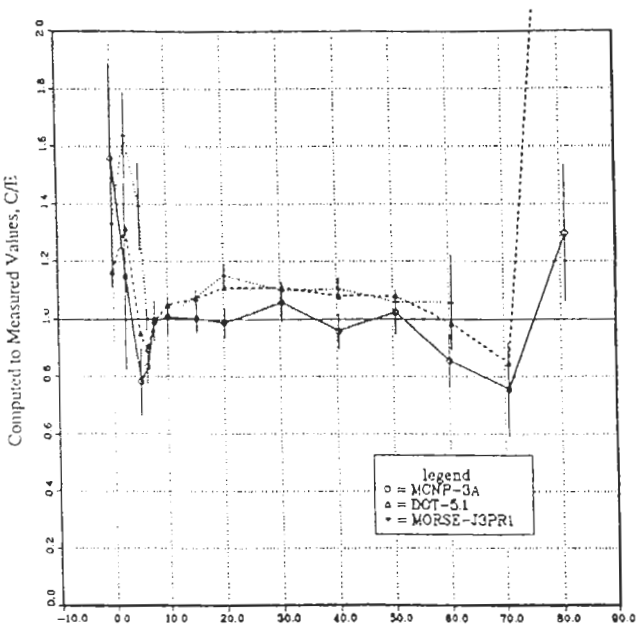

Fig. (5) The C/E values for tritium production rate from ^{6}Li, T_6, along the central axis of the Be-front system of Phase IIA

VI.1.B TRITIUM PRODUCTION RATE FOR ^{7}Li (T_7)

The C/E values for T_7 in the reference system along the central axis as obtained by the U.S., are generally larger (DOT4.3: C/E = 1.1-1.2; MCNP: C/E = 1-1.2) than the values obtained by JAERI (DOT 3.5: 1.1-0.9; MORSE: 1.1-0.8). It was shown that the $^{7}Li(n,n'\alpha)t$ cross-section as currently implemented in JENDL3-PR1 is underestimated by 8-10% as compared to Young's evaluation.[15] In addition, one notices a falling slope in the C/E curves obtained by JAERI where values fall below unity at depth 20-30 cm inside the Li_2O zone [see Fig. (6) for the Be-front system]. Direct comparison of the various cross-sections for ^{7}Li in JENDL3-PR1 and Young's evaluation showed that the ^{7}Li(n, total) cross-section is overestimated in JENDL3-PR1 due to overestimation in $^{7}Li(n,elastic)$, $^{7}Li(n,\gamma)$ and $^{7}Li(n,d)$ cross-sections as discussed in Ref. (6). The overmoderation due to $^{7}Li(n,elastic)$ scattering (by ~4%) and neutrons disappearance due to $^{7}Li(n,\gamma)$ and $^{7}Li(n,d)$ reactions lead to the slope shown in Fig. (6) in JAERI's calculation at deeper locations. This feature is also apparent for the threshold-type reaction rates such as $^{27}Al(n,\alpha)^{24}Na$, where the C/E values tend to decrease by depth in the Li_2O zone in JAERI's calculations while the U.S. values are in general relatively constant (C/E ~0.98-1.08). The C/E values for T_7 in the Be-sandwiched system is similar in features to those shown in Fig. (6).

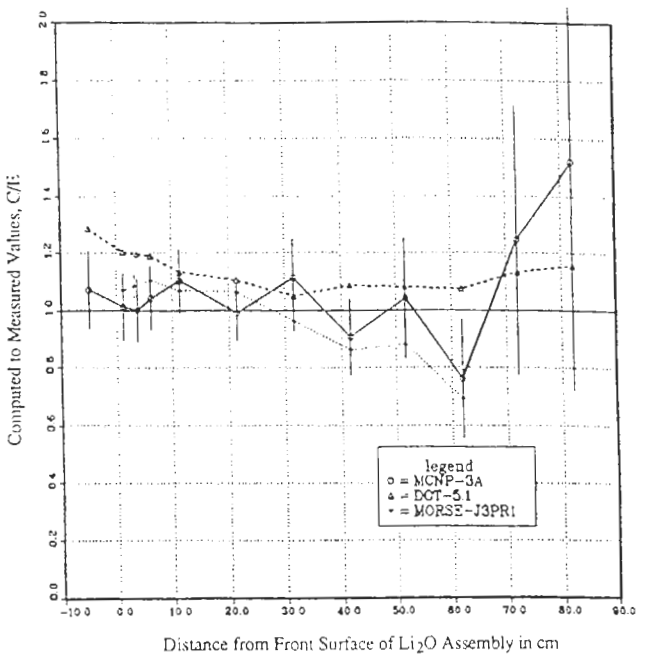

Fig. (6) The C/E values for tritium production rate from ^{7}Li,T_7, along the central axis of the Be-front system of Phase IIA

IV.1.C ZONAL TRITIUM PRODUCTION RATE

The TPR from natural lithium, ^{6}Li, and ^{7}Li, were measured in zones selected along the central drawer in the reference and the Be-sandwiched systems. The C/E values for T_N in the reference system are 1.02-1.2 (DOT3.5), 1.09-1.1 (DOT4.3), 0.85 - 1.2 (MCNP) and 0.99 - 1.2 (MORSE-DD) [See Fig. (7)]. In the Be-sandwiched system, the C/E values are 0.99 - 1.09 (DOT5.1), 0.83-1.29 (MCNP) and 0.95-1.05 (MORSE-DD). The C/E values for zonal T_7 were shown to be less than unity in the reference case (C/E ~0.73 - 0.93).

The measured and calculated zonal TPR from natural Li are given in Table 1-a for the reference and the Be-sandwiched systems. The values shown are integrated results over the entire volume of the central drawer (~5.08 x 5.08 x 60 cm) per atom of natural Li per source neutron. Values in parentheses are the relative values with respect to the reference system and thus indicate the tritium breeding potential in the central drawer. As shown, the TPR from natural Li in the Be-sandwiched system has been increased by ~8% as predicted by MCNP. The predicted increase by DOT5.1 (U.S.) is ~7% and the MORSE-DD calculations indicate a similar increase. However, the experimentally measured increase in the TPR is ~10%. Table (1)-b shows the C/E values for the integrated zonal TPR in both systems. As shown, MCNP results are lower than measurements by ~1-3% in both systems, while MORSE results are larger by 3% and lower by 1% in the reference and Be-sandwiched system, respectively. The DOT results, however, are larger by 7% and 4% in the two systems.

IV.2 PHASE IIB

IV.2.A EFFECT OF BERYLLIUM LINER/FRONT LAYER ON T_6 PROFILES

The inclusion of a 5 cm-thick beryllium liner on the inner surface of the Li_2CO_3 enclosure tends to soften the incident spectrum at the entrance of the Li_2O assembly and hence an increase in T_6 occurs as depicted in Fig. (8) which shows the ratio of the local T_6 along the central axis in the reference and the Be-front (W/o FW) systems of Phase IIB to the corresponding values in Phase IIA (no Be liner). The ratios shown (enhancement factors, M_6) are those predicted by the

Table (1): Integrated zonal TPR from natural lithium in the reference and the Be-sandwiched systems of Phase IIA

a. Increase in the tritium breeding potential

Method	Reference	Be-sandwiched
MCNP(U.S.)	2.442-28* (1.0)	2.644-28+ (1.083)
DOT (U.S.)	2.657-28 (1.0)	2.832-28+ (1.066)
MORSE (JAERI)	2.541-28 (1.0)	2.727-28+ (1.073)
Measurement	2.477-28 (1.0)	2.732-28+ (1.103)

b. C/E Values

Method	Reference	Be-sandwiched
MCNP (U.S.)	0.986	0.968
DOT (U.S.)	1.073	1.037
MORSE (JAERI)	1.026	0.998

* Units: Tritium atom/natural Li atom/source neutron

+ Tritium produced in the beryllium zone is excluded

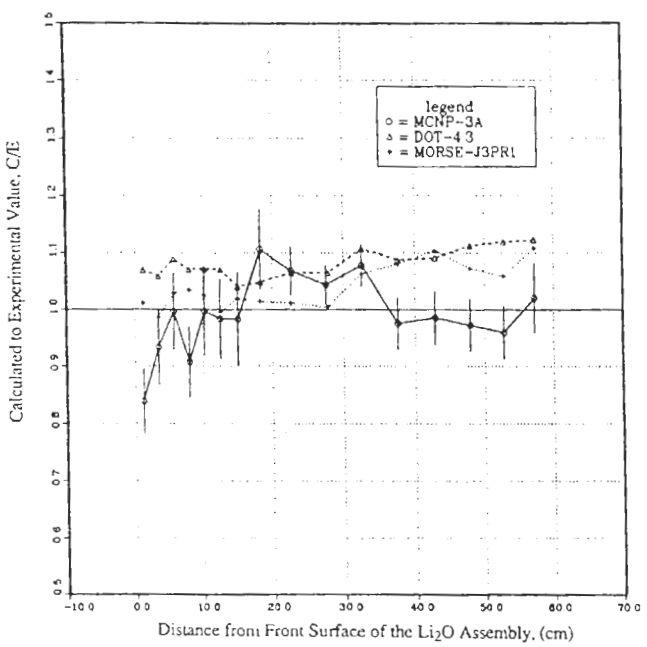

Fig. (7) The C/E values for zonal tritium production rate from natural lithium in the reference system of Phase IIA

DOT5.1 calculations, M_6^C, and measured by the Li-glass detectors, M_6^E. In the reference system, the enhancement factor at the front surface is $M_6^E = 23$ while the enhancement factor is $M_6^C = 14$ as predicted by the DOT calculations. Note that the low-energy component of the incident spectrum gets absorbed rapidly by ^{6}Li throughout the first 10-20 cm inside the assembly and the ratio M_6 is close to unity at deeper locations. In the Be-front system, the inclusion of the Be-liner tends to further increase T_6 behind the front Be layer but the local increase at these locations is less pronounced than in the reference system. However, since the incident spectrum gets further softened inside the front Be layer, a remarkable increase in T_6 occurs inside this layer [by a factor of ~21(DOT) and a factor of ~17 (measurements)].

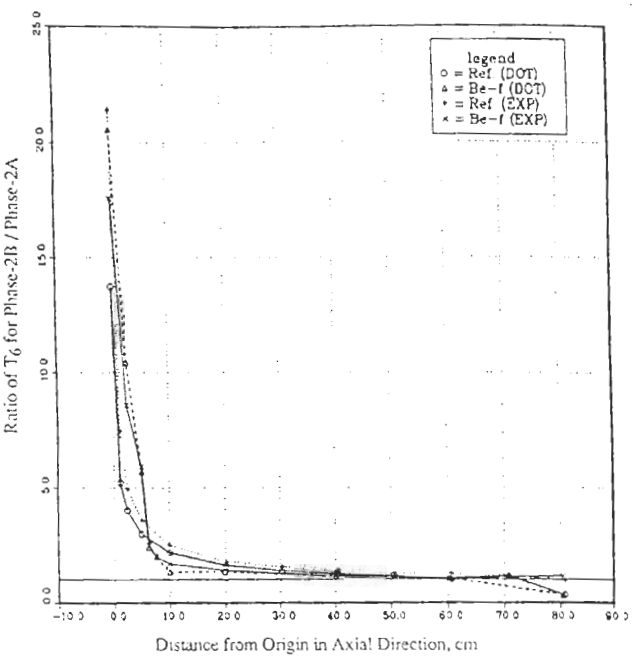

Fig. (8) Ratios of local T_6 in the reference and the Be-front system of Phase IIB with a Be-liner to the corresponding values without a Be-liner (Phase IIA) (measurements by Li-glass detectors)

The C/E values in the reference and the Be-front system (w/ FW) are shown in Fig. (9) and (10), respectively. The C/E values as calculated by the U.S. are lower than unity at the front surface of the Li_2O assembly in the reference system (MCNP: C/E = 0.63, DOT5.1: C/E = 0.72) while the values obtained by JAERI are larger (MORSE-DD: C/E=1, DOT3.5: C/E = 1.23). This could be attributed to the observation made earlier that in Young's evaluation for the Be(n, 2n) reaction at high energies the emission spectrum has a low energy component (E<0.5 MeV) in comparison to the JENDL-3PR1 evaluation. Therefore, neutrons interacting with the Be liner and reflected toward the test assembly in JAERI's calculation have a larger component below 0.5 MeV which leads to larger T_6 at the front locations. For the same reason, the C/E values inside the Be-front layer are also larger in JAERI's calculations as can be seen from Figs. (5) and (10). It can also be seen from Fig. (10) that the C/E values obtained by JAERI are larger at the front surface of the Be layer and lower just behind this layer than the values obtained by the U.S. This could be explained by the observation made by Takahashi[20] who showed that the angular distribution of the ^{9}Be(n,2n) cross-section of JENDL3 is overestimated in the backward direction and underestimated in the forward direction. In the bulk of the Li_2O, however, the C/E values are 1 -1.18 (U.S.) and 0.8-0.9 (JAERI) in the reference system and are 1-1.15 (U.S.) and 0.93-1 (JAERI) in the Be-front system. The large C/E values inside the Be layer are due to the self-shielding effect and flux perturbation by the Li-glass detector as explained earlier in Section IV.1. Note also from Figs. (5) and (10) that the C/E values fall below unity just behind the front Be layer, and then sharply rise after 3-5 cm to reach more or less steady values and then decrease toward the back locations. These features are related to the beryllium cross-sections as explained below.

One notices from Fig. (8) that the enhancement factors M_6^C are always less than M_6^E except inside the beryllium zone in the Be-front

system, that is, the calculations underestimate the local increase in T_6 in the Li_2O assembly in the reference system and behind the Be layer in the Be-front system. This is further illustrated in Fig. (11) which shows the ratios M_6^C/M_6^E in both systems. The enhancement in T_6 is underestimated by ~35% at the front surface in the reference system and the discrepancy between M_6^C and M_6^E gets less in the bulk of the Li_2O assembly. These features are the same behind the Be zone in the Be-front system but the discrepancy is less pronounced. Note that the ratio M_6^C/M_6^E is equal to the ratio of C/E values in each system of Phase IIB to the C/E values of that system in Phase IIA.

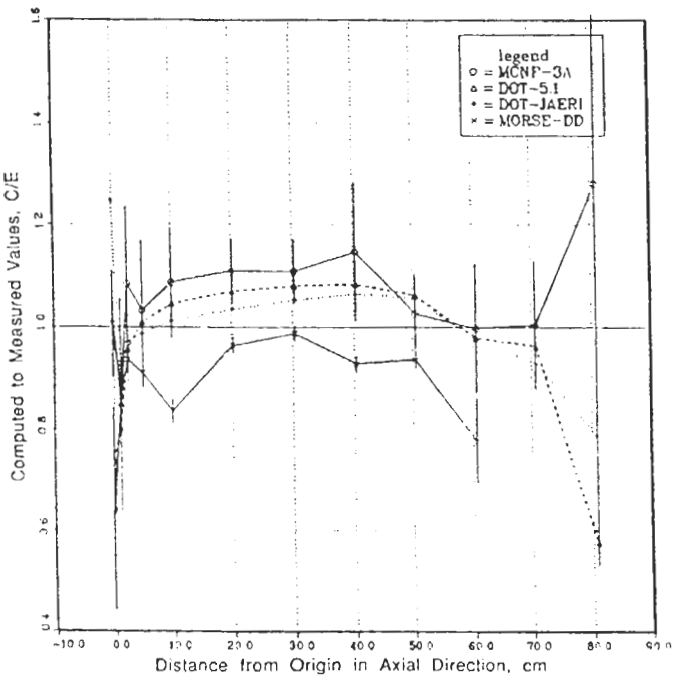

Fig. (9) The C/E values for tritium production rate from ^6Li, T_6, along the central axis of the reference system of Phase IIB

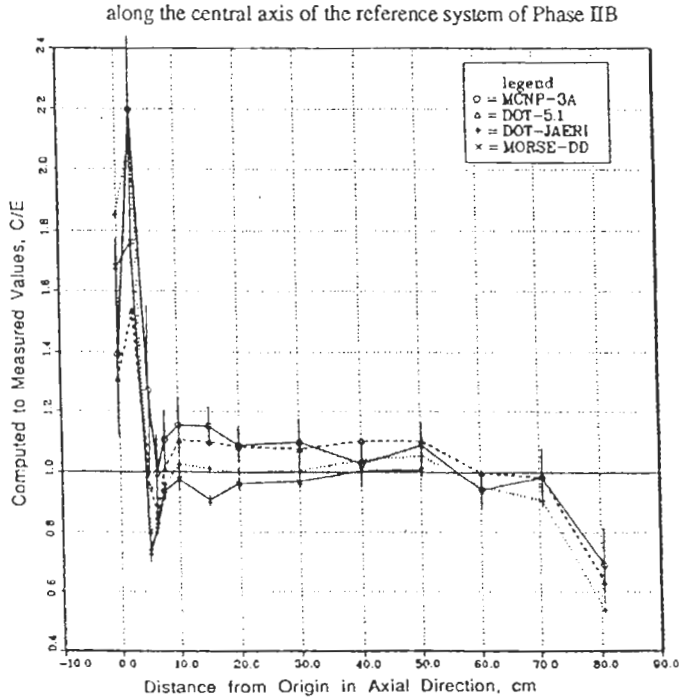

Fig. (10) The C/E values for tritium production rate from ^6Li, T_6, along the central axis of the Be-front system (w/FW) of Phase IIB

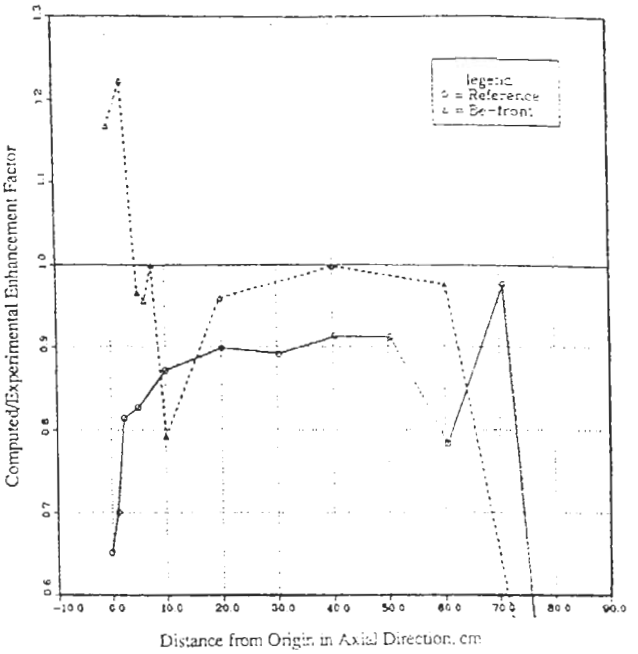

Fig. (11) The ratios of the computed to the experimental values of the enhancement factor for T_6, M_6, in Phase IIB due to the inclusion of the Be-liner

The reason for the above mentioned features could be explained by comparing the computed enhancement factor M_6^C (ratio of the local T_6 in the case where a Be layer is included to the corresponding value in the reference system) to the measured one, M_6^E, in the Be-front and Be-sandwiched systems of Phase IIA and in the Be-front system of Phase IIB, as shown in Fig. (12). It is clear from the figure that M_6^C/M_6^E is always less than unity in the Li_2O zone(s) of Phase IIA and that the discrepancy is more pronounced just behind the Be layer. Note from Fig. (12) the similarity (in shape) to the C/E curves shown in Figs. (5) and (10). The enhancement in T_6 is underestimated by ~30% behind the Be layer and by ~10% in the bulk of the Li_2O zone in both systems of Phase IIA. The range of this discrepancy is similar to the one shown in Fig. (11) due to the inclusion of the Be liner in the reference system. In Phase IIB, the discrepancy in the enhancement factor between calculations (DOT5.1) and measurement upon including a front Be layer is less pronounced and is ~20% behind the Be layer and ~2% in the bulk of the Li_2O zone, as shown in Fig. (12). These features could be explained if the emerging neutrons from the Be layer are underestimated in the low-energy range (below 0.5 MeV) and overestimated in the energy range 2-10 MeV. The underestimation in the low-energy component leads to the large discrepancy in the enhancement factor just behind the Be layer. However, the overestimation in the emerged neutrons in the energy range 2 MeV < E < 10 MeV tends to improve the discrepancy since these neutrons are slowed down as they travel inside the Li_2O zone, and thus lead to an increase in the local values of T_6 by distance and the discrepancy caused by the underestimation in the emerged spectrum below 0.5 MeV tends to decrease.

Oyama and Maekawa[21] have shown that the spectrum of the emerged neutrons from a 5 cm-thick beryllium slab is indeed underestimated in the energy range 0.1-0.5 MeV upon using LANL, JENDL3-PR1, and ENDF/B-IV data for beryllium. They have also shown that this spectrum is overestimated in the energy range 2-10 MeV with LANL (Young's) evaluation by ~10-20% but is underestimated by ~20-40% with the JENDL3-PR1 evaluation while the spectrum above 10 MeV is underestimated by 20-30% with both evaluations. Since the $^9Be(n,2n)$ reactions are appreciable inside the Be layer, one can suspect that the emission spectrum from these reactions is underestimated in the energy range below 0.5 MeV and overestimated

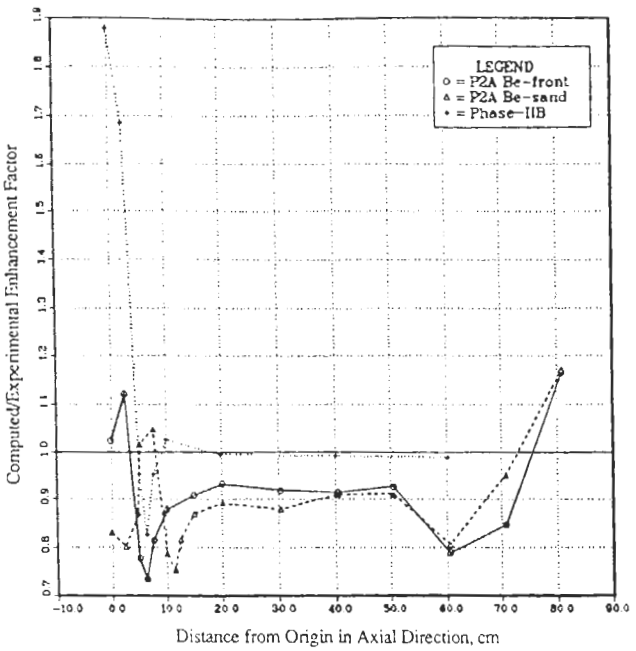

Fig. (12) The ratios of the computed to the experimental values of the enhancement factor T_6, M_6, in Phase IIA and IIB due to the inclusion of the Be-layer

(in Young's evaluation) in the energy range 2 MeV < E < 10 MeV. Since more such interactions occur if the incident spectrum is hard (as in Phase IIA), the discrepancy in the computed and measured enhancement factor for T_6 is more pronounced in Phase IIA than in Phase IIB behind the front Be layer, as shown in Fig. (12).

The fact that the enhancement in T_6 upon including the Be liner in Phase IIB is also underestimated, as shown in Fig. (11), is consistent with the results of Oyama and Maekawa's experiment. Neutrons emitted from the ^{9}Be(n,2n) reactions in the Be-liner and reflected toward the test assembly could be underestimated in the energy range below 0.5 MeV and overestimated in the energy range 2 MeV < E < 10 MeV. The overestimation of the incident spectrum in the energy range 2 MeV < En < 10 MeV could be seen from Fig. (13) which shows comparison to the measured spectrum by NE213 measurements at the surface of the Li_2O assembly in the reference system of Phase IIB. Note that NE213 measurements below 1 MeV are not reliable due to the inherent inaccuracy of this method below this energy.

IV.2.B EFFECT OF BERYLLIUM LINER/FRONT LAYER ON T_7 PROFILES

The ratios of the local T_7 in the cases where a Be liner on the inner surface of the Li_2CO_3 enclosure is included to the corresponding values without a liner in the reference and the Be-front system are shown in Fig. (14) as determined by calculations (DOT5.1, U.S.) and by measurements (NE213 indirect method). While DOT calculations predict an increase in T_7 of 2-5% up to 10 cm-depth in the reference system and a decrease of 2-10% thereafter, measurements indicate an increase of 10-15% throughout the entire Li_2O zone. In the Be-front system (w/o FW) the predicted change is similar to the reference system but measurements show an increase of 5-15%. The ratio of the computed enhancement factor, M_7^C, to the measured one, M_7^E, is shown in Fig. (15) for the two systems. As for T_6, the enhancement factor is underestimated by calculations throughout the entire test assembly and the underestimation is larger in the reference system in comparison to the Be-front system.

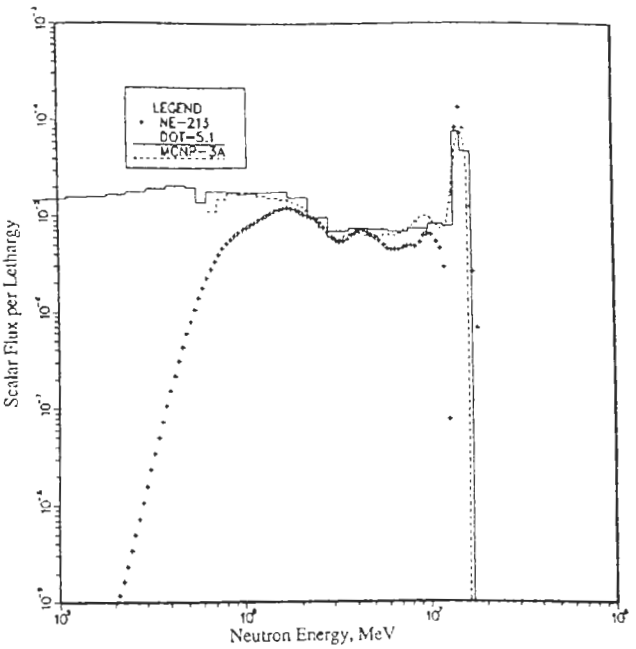

Fig. (13) Neutron spectrum at the entrance of the Li_2O assembly (z=0) in the reference system of Phase IIB

As was shown in Fig. (12) for T_6, the ratios of the computed enhancement (or rather a decrease) factor, M_7^C, (ratio of local T_7 in the case where a Be layer is included to the corresponding value in the reference system) to the measured one, M_7^E, in the Be-front and Be-sandwiched systems of Phase IIA and in the Be-front system (w/o FW) of Phase IIB are shown in Fig. (16). As shown, these ratios are always less than unity throughout the Li_2O zone in both systems of Phase IIA but slightly larger than unity inside the Be layer. Thus, the calculations overestimate the relative decrease in local T_7 inside the Li_2O zone (or underestimate T_7) upon the inclusion of the Be layer. (The Be layer acts as a moderator and hence local T_7 are decreased in the Li_2O zone). Similar features were found in the Be-front system of Phase IIB, as also shown in Fig. (16).

The underestimation in the local T_7 upon including the Be layer could be related to the accuracy of the total ^{9}Be(n,2n) cross-section as currently implemented in LANL and JENDL-3PR1 evaluations. This cross-section is overestimated in these evaluations above 10 MeV and therefore neutron moderation at high energy throughout ^{9}Be(n,2n) reactions are overestimated. This is supported by the observation made by Oyama and Maekawa in their experiment where the emerged spectrum from the 5 cm-thick Be slab is underestimated above 10 MeV. This can also be seen from Fig. (17) that shows a comparison of the calculated neutron spectrum behind the Be layer in the Be-front system (w/ FW) of Phase IIB where the 14 MeV peak is underestimated by calculations. The underestimation of the 14 MeV peak can also be seen in Fig. (13) due to the collisions in the Be liner where overestimation in the ^{9}Be(n,2n) reactions exists. The underestimation in the 14 MeV peak was observed in all the spectra that were measured at various locations inside the assembly in Phase IIB. One can also notice in Fig. (16) that the discrepancy between M_7^C and M_7^E gets larger at the back locations since the effect of the underestimation in the high-energy component of the emerged neutrons from the Be-layer is more pronounced at deep locations. Furthermore, cross-section sensitivity analysis has indicated that T_7 has negative sensitivity coefficient to an increase in the Be(n,2n) cross-section at high-energy and that this coefficient gets larger as one proceeds deeper into the Li_2O zone behind the Be layer. Since less ^{9}Be(n,2n) reactions occur if the incident spectrum is soft, the discrepancy between M_7^C and M_7^E is smaller in Phase IIB.

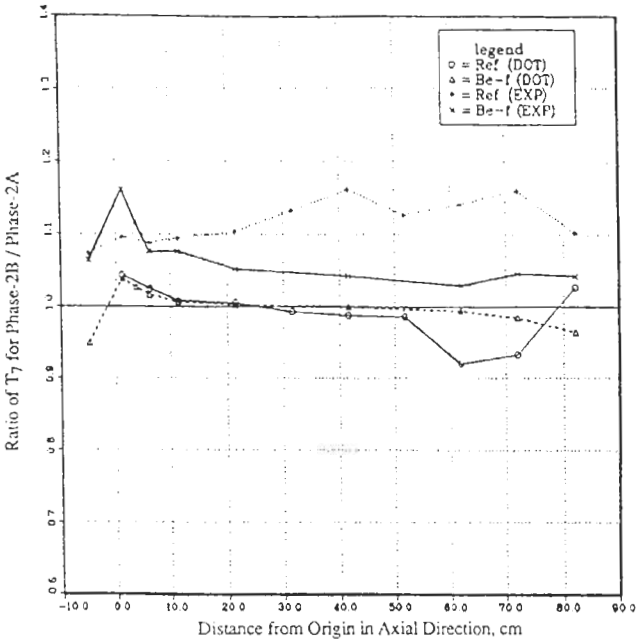

Fig. (14) Ratios of local T_7 in the reference and the Be-front systems of Phase IIB with a Be-liner to the corresponding values without a Be-liner (Phase IIA)

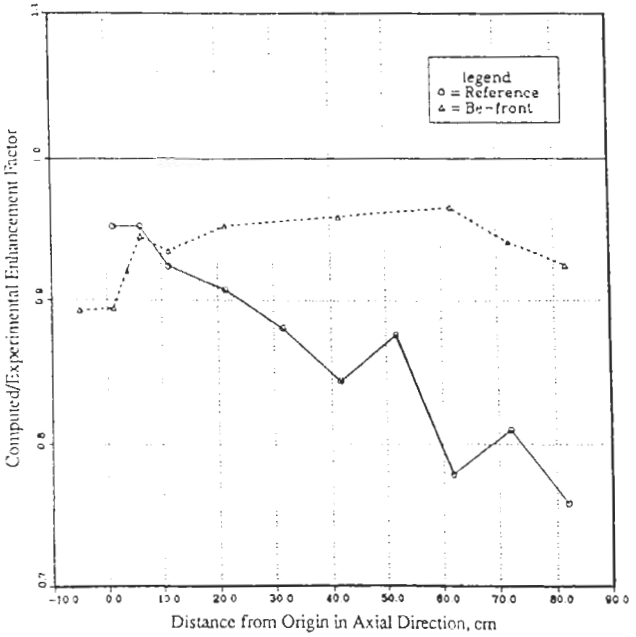

Fig. (15) Ratios of the computed to the experimental values of the enhancement factor for T_7, M_7, in Phase IIB due to the inclusion of the Be-liner

The overestimation in the relative decrease in T_7 upon including a front Be layer in Phase IIA and the underestimation in the enhancement factor for T_6 lead to underestimation in the enhancement in tritium breeding upon including the beryllium multiplier. This is supported by the results shown in Table (1) where calculations underestimate the enhancement in the integrated zonal TPR by ~3% relative to measurements. Note that this underestimation is for the natural Li_2O breeder and the results could be different for other breeding materials that are enriched in ^6Li. Also, the overestimation in the relative decrease in local T_7 upon including a Be liner in Phase IIB [see Fig. (15)] and the underestimation in the enhancement factor for local T_6 in that phase [see Fig. (11)] lead to underestimation in the integrated values throughout the Li_2O zone. Based on the Li-glass and NE213 measurements, line integrated TPR from ^6Li, ^7Li, and Li(natural) throughout the central drawer (5.06 x 5.06 x 60 cm) were estimated in the reference and Be front systems (w/FW) and comparison was made to the integrated experimental values. The result from such a comparison is shown in Table (2) based on the MORSE-DD results (JAERI). As shown, the integrated TPR are always underestimated, particularly in the Be-front system by as much as 12% (for T_N). This is basically due to the underestimation in T_6, particularly in the 3-5 cm zone behind the Be layer which contributes by ~50% to the total integrated TPR.

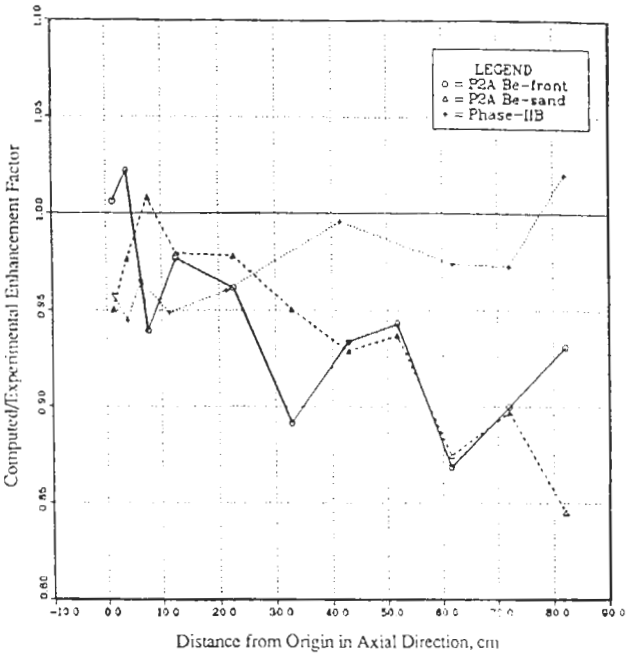

Fig. (16) Ratios of the computed to the experimental values of the enhancement factor for T_7, M_7, in Phase IIA and IIB due to the inclusion of the Be-layer

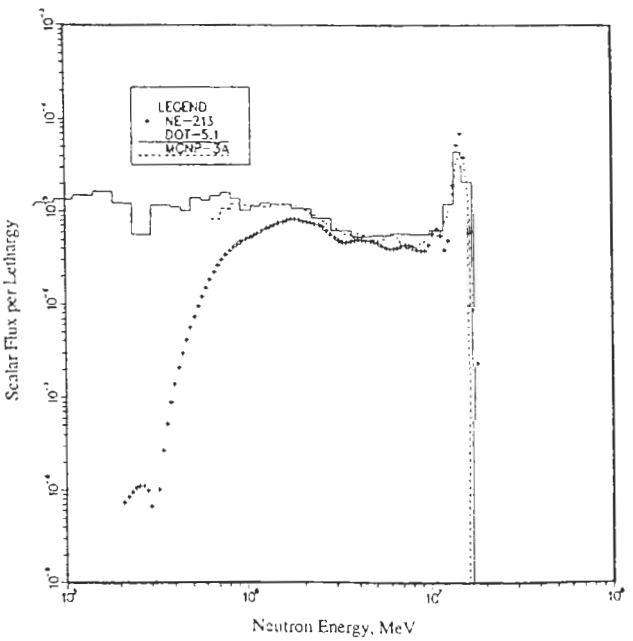

Fig. (17) Neutron spectrum behind the front Be layer at z=5 in the Be-front system (w/FW) of Phase IIB.

Table (2) Line Integrated TPR (10^{-24} * tritium/source*neutron) in Phase IIB Experiments

REF	Exp.	Calc.	C/E
T_7	9.34-5	9.02-5	0.97
T_6	5.49-3	5.02-3	0.91
T_N	4.93-4	4.55-2	0.93
BEF(w/FW)	Exp.	Calc	C/E
T_7	5.87-5	5.53-5	0.94
T_6	4.45-3	3.93-3	0.88
T_N	3.84-4	3.42-4	0.89

IV.2.C. IN-SYSTEM REACTION RATES DISTRIBUTION

The comparisons between the predictions of several reaction rates distributions inside the test zone to the foil activation measurements were useful in supporting the observations made above regarding the adequacy of beryllium cross-sections. It was shown that the C/E values for the ^{58}Ni(n,2n) reactions ($E_{th} \cong$ 13 MeV) fall below unity in JAERI's calculations behind the front Be-layer (although Ikeda et al.'s reliable cross-section was used in these calculations) and are ~0.8-0.9 in the bulk of the Li_2O zone. Overestimation in the ^{9}Be(n,2n) reactions inside the Be layer could lead to a decrease in the ^{58}Ni(n,2n) reaction due to the decrease in the high-energy component (above 10 MeV) of neutrons emerging from that layer. The C/E values obtained by the U.S. show similar trends but they are smaller (C/E=0.75-0.8) due to the smaller ^{58}Ni(n,2n) cross-section implemented in ENDF/B-V which needs reevaluation. The fall in the C/E curves behind the Be-layer appears in all other high threshold reactions, as shown in Fig. (18) for ^{93}Nb(n,2n) reactions ($E_{th} \cong$ 8 MeV) where the C/E values in the bulk of the Li_2O zone are less than unity (~0.9) in all the calculations. For the ^{197}Au(n,γ) reactions that are sensitive to the low energy component of neutrons, it was shown that the C/E curves obtained by JAERI and the U.S. have the same trends which are similar to the C/E curves for T_6.

V. SUMMARY

Useful information on the adequacy of the cross-sections of several materials was obtained from the integral experiments performed in Phase II of the U.S./JAERI Collaborative Program on Fusion Blanket Neutronics. Examples are a) the recently measured cross-sections by Ikeda, et al., for ^{58}Ni(n,2n), ^{58}Ni(n,p)...etc., give better agreement with the measured values for the corresponding reaction rates than the cross-sections currently implemented in JENDL-3 file. The ^{58}Ni(n,p) cross-section of ENDF/B-V is adequate but the ^{58}Ni(n,2n) cross-section is underestimated by 10-20%; b) the ^{7}Li (n, total) cross-section in JENDL-3PR1 is overestimated due to the overestimation in ^{7}Li(n,elastic), ^{7}Li(n,γ) and ^{7}Li(n,d) cross-sections and that ^{7}Li(n,n'α)t cross-section is underestimated by 8-10% in comparison to Young's evaluation; c) the ^{9}Be(n,2n) cross-section is both JENDL-3PR1 and Young's evaluation is overestimated at high energies, which has a consequent impact on underestimating high-energy reactions behind the beryllium multiplier such as T_7, ^{58}Ni(n,2n), etc., and d) there are indications that the emission spectrum from the ^{9}Be(n,2n) reactions seems to be underestimated below 0.5 MeV and underestimated above 10 MeV in both evaluations and is overestimated in the energy range 2 MeV-10 MeV in Young's evaluation.

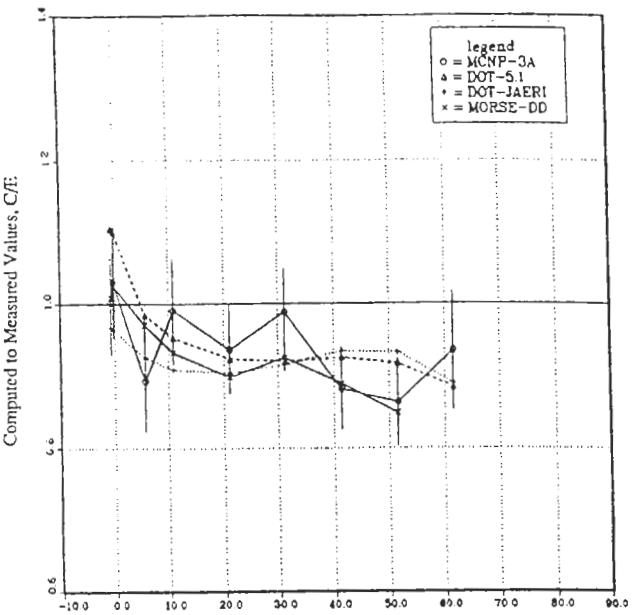

Fig. (18) The C/E values for ^{93}Nb(n,2n) reaction along the central axis of the Be-front system (w/ FW) of Phase IIB

It was also shown that the inadequacy in the beryllium data leads to underestimating the enhancement in tritium breeding potential upon including beryllium as a neutron multiplier. This underestimation could be a characteristic of the natural Li_2O breeding material used in the experiments and the results may be different for other breeders that are enriched in ^{6}Li.

ACKNOWLEDGEMENT

The U.S. effort in this collaborative program is supported by the United States Department of Energy, Office of Fusion Energy under Grant No. DE-F603-86ER52124.

REFERENCES

1. T. NAKAMURA and M.A. ABDOU, "Summary of Recent Results from the JAERI/U.S. Fusion Neutronics Phase I Experiments. Fusion Technol., 10, 541-548 (1986)

2. M. Z. YOUSSEF, et al., "Analysis and Intercomparison for Phase I Fusion Integral Experiments at the FNS Facility," Fusion Technol., 10, 549-563 (1986)

3. M. Z. YOUSSEF, M. NAKAGAWA, et al. "Phase I Fusion Integral Experiments, Vol. II: Analysis," UCLA-ENG-88-15, University of California, Los Angeles, (September 1988). See also JAERI-M-88-177, Japan Atomic Energy Research Institute (Aug. 1988).

4. H. MAEKAWA, et al., "Measured Neutron Parameters for Phase I Experiments at the FNS Facility," Fusion Technol., 10, 564-572 (1986)

5. M. NAKAGAWA, et al., "Analysis of Neutronics Parameters Measured in Phase II Experiments of the JAERI/U.S. Collaborative Program on Breeder Neutronics, Part I: Source Characteristics and Reaction Rate Distributions," Proc. of the International Symposium on Fusion Nuclear Technology, April 10-15, Tokyo, Japan (1988). To appear in Fusion Engineering and Design.

6. M. Z. YOUSSEF, et al., "Analysis of Neutronics Parameters Measured in Phase II Experiments of the JAERI/U.S. Collaborative Program on Blanket Neutronics, Part II: Tritium Production and In-System Spectrum," Proc. of the International Symposium on Fusion Nuclear Technology, April 10-15, Tokyo, Japan (1988). To appear in Fusion Engineering and Design.

7. T. NAKAMURA and M. A. ABDOU, "Overview of JAERI/U.S. DOE Collaborative Program on Fusion Blanket Neutronics Experiments,"Proc. of the International Symposium on Fusion Nuclear Technology, April 10-15, Tokyo, Japan (1988). To appear in Fusion Engineering and Design.

8. T. NAKAMURA, et al., "A Study of Testing Models for the Blanket Neutronics Experiments," this issue.

9. Y. OYAMA, et al., "Phase IIB Experiment of JAERI/U.S.DOE Collaborative Program on Fusion Blanket Neutronics," This issue.

10. Y. IKEDA, et al, "Determination of Neutron Spectrum in D-T Fusion Field by Foil Activation Technique," this issue.

11. A. KUMAR, et al," Analysis for the Selection of Experimental Configurations for Heterogeneity and Be-Multi-layered Experiments of U.S./JAERI Collaborative Program on Blanket Neutronics," this issue.

12. LOS ALAMOS MONTE CARLO GROUP, "MCNP--A General Monte Carlo Code for Neutron and Photon Transport," version 3A, LA-7396, Rev. 2, Los Alamos National Laboratory (1986)

13. M. NAKAGAWA and T. Mori, "MORSE--DD, A Monte Carlo Code Using Multigroup Double Differential Form Cross-Sections" JAERI-M84-126, Japan Atomic Energy Research Institute (July 1984)

14. R. MACFARLANE, "TRANSX-CTR: A Code for Interfacing MATXS Cross-Section Libraries to Nuclear Transport Codes for Fusion Systems Analysis," LA-9863-MS, Los Alamos National Laboratory (February 1984)

15. P.G. YOUNG, "Evaluation of n+^{7}Li Reactions using Variance-Covariance Techniques," Trans. Am. Nucl. Soc., 39, 272 (1980)

16. P. G. YOUNG and L. STEWART, "Evaluated Data for n+^{9}Be Reactions" LA-7932-MS(ENDF-283), Los Alamos National Laboratory. (1979)

17. R. T. SANTORO, et al., ORACT: 174-Neutron-Group Activation Cross-Section Library for Fusion and Fission Reactor Design Studies, Oak Ridge National Laboratory, ORNL/TM-9203 (June 1984)

18. Y. IKEDA, et al., "Measurement of High Threshold Activation Cross-sections for 13.5 to 15 MeV Neutron," Proc. Int. Conf. on Nuclear Data for Basic and Applied Science, Santa Fe, New Mexico, (1985). See also JAERI-1312, Japan Atomic Energy Research Institute, March (1988)

19. J. BENVENISTE, et al., "The Problem of Measuring the Absolute Yield of 14-MeV Neutrons by Means of an Alpha Counter," Nucl. Instrum. Method, 7, 306-314. (1960)

20. A. TAKAHASHI, "Differential Neutron Emission Data and JENDL-3 for Multiplier and Structural Materials," presented at the U.S./Japanese Universities Workshop on Fusion Neutronics, University of California, Los Angeles, January 25-29. (1988)

21. Y. OYAMA AND H. MAEKAWA, "Measurements and Analysis of an Angular Neutron Flux on a Beryllium Slab Irradiated with Deuterium-Tritium Neutrons, Nucl. Sci. & Eng., 97, 220-234 (1987)